EPJ Web of Conferences **242**, 03001 (2020) https://doi.org/10.1051/epjconf/202024203001
FPY 2019

Microscopic Calculation of Fission Fragment Distributions in Actinides

N. Schunck[1]*

[1]Nuclear and Chemical Sciences Division, Lawrence Livermore National Laboratory, Livermore, CA 94551, USA

Abstract. The simulation of independent and cumulative yields requires precise knowledge of the initial conditions of the fission fragments immediately after scission. In this paper, we use a quantum-mechanical description of fission dynamics to extract the initial mass distribution of fission fragments for the neutron-induced fission of the two major actinides ^{239}Pu and ^{235}U, both for thermal fission and as a function of the incident neutron energy.

1 Introduction

Nuclear fission remains a fascinating basic science problem, which challenges our understanding of both nuclear forces and the structure of interacting quantum many-body fermion systems. A lot of progress has been made to build a microscopic description of this process, where fission observables would be computed within a fully quantum-mechanical theory [1]. Nuclear density functional theory (DFT) is currently the most natural framework to achieve this, as it is naturally tailored to handle heavy nuclei for which most experimental data on fission is available [2]. As we progress in the path to building a comprehensive, predictive theory of fission, it is important to establish a number of reference points along the way.

The goal of this paper is precisely to report such benchmark calculations. In this paper, we are going to focus on the initial fission fragment mass distributions (before prompt emission) for the particular cases of ^{239}Pu(n,f) and ^{235}U(n,f). In addition to results for thermal fission, we are also going to show results as a function of the incident energy of the neutron. In Section 2, we briefly recall the theoretical framework that we used while results are presented in Section 3.

2 Theoretical Framework

The charge and mass distributions of fission fragments are extracted by explicit simulation of fission dynamics within a fully quantum-mechanical framework. Specifically, we work within the time-dependent generator coordinate method (TDGCM) under the Gaussian overlap approximation (GOA). As discussed in details in [3–10], the GOA allows recasting the Hill-Wheeler equation of the TDGCM into a collective, Schrödinger-like equation of motion for a collective wave package $g(\boldsymbol{q}, t)$ in the multi-dimensional collective space C spanned by collective variables $\boldsymbol{q}$. In practice, we used the code FELIX-2 to solve the collective Schrödinger

*e-mail: schunck1@llnl.gov

equation and extract the fission fragment distributions $Y(A)$ from the flux of the wave packet through the scission line; for details about the general methodology, see [9].

The collective space C is generated by solving the HFB equation with constraints on the expectation value of the axial quadupole and axial octupole moments, $\boldsymbol{q} \equiv (q_{20}, q_{30})$. All HFB calculations have been performed with the SkM* parametrization [11] of the Skyrme energy density functional. The pairing channel is described with a surface-volume, density-dependent pairing force. The strengths $V_{0,n}$ and $V_{0,p}$ of this interaction were fitted in each nucleus of interest in order that the HFB pairing gap in the ground-state reproduce the experimental value of the 3-point odd-even staggering indicator [12]. For ^{240}Pu, this gives: $V_{0,n} = -265.250$ MeV and $V_{0,p} = -340.062$ MeV, and for ^{236}U: $V_{0,n} = -255.250$ MeV and $V_{0,p} = -325.594$ MeV. The HFB equation is solved with the HFODD solver by expanding the solutions on the one-center harmonic oscillator (HO) basis [13]. We used the exact same characteristics as in [14].

The practical implementation of the TDGCM+GOA also requires the knowledge of the collective inertia, or mass, tensor $\mathsf{B}(\boldsymbol{q})$, the metric tensor $\gamma(\boldsymbol{q})$, and the zero-point energy correction $\varepsilon_{\mathrm{ZPE}}(\boldsymbol{q})$. All these quantities were computed from the GCM formula at the perturbative cranking approximation; see Chap. 6 in [2] for details. This choice was made in order to guarantee consistency between all the ingredients of the model.

3 Benchmark Results

We focus on the neutron-induced fission of the two major actinides, ^{239}Pu and ^{235}U, which both lead to an even-even compound nucleus. For each of these two nuclei, we compute the potential energy surface (PES) in the two-dimensional collective space C spanned by collective variables $\boldsymbol{q} \equiv (q_{20}, q_{30})$, where $q_{\lambda\mu}$ is the expectation value of the mass multipole moment of multipolarity λ, μ on the HFB wavefunction. An example of the potential energy surface for ^{236}U is shown in Fig.1; the results for ^{240}Pu are shown in [14]).

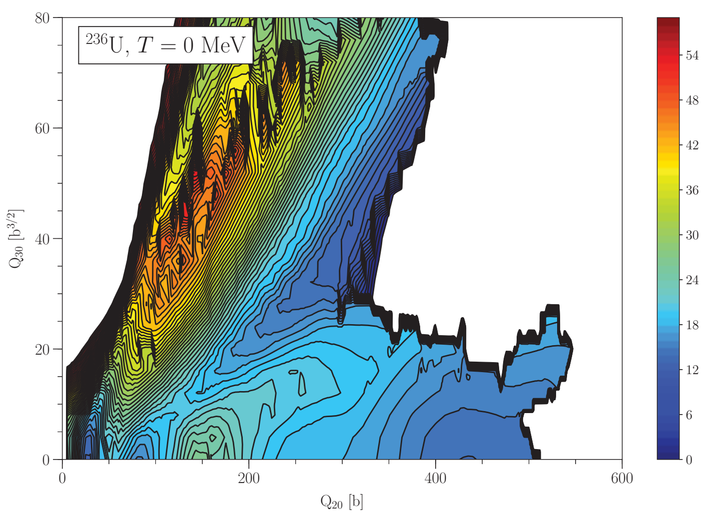

Figure 1. Two-dimensional potential energy surface for ^{236}U. The energy is computed at the HFB level with the SkM* Skyrme functional and the pairing force as described in the text.

In this benchmark, we define scission configurations by the condition that the expectation value of the Gaussian neck operator is lower than $q_{\rm cut}$. Since there is a considerable amount of ambiguity on the actual definition of scission – see discussion in [1, 14, 15] and references therein, we look at three possible choices $q_{\rm cut} = 4, 5$ and 6. Given this definition, the PES and the collective mass tensor associated with each point of said PES, we run the code FELIX and solve the collective Schrödinger-like equation for collective dynamics. To guarantee convergence of the results, we adopt a finite-element grid characterized by $h = 6$ and run the solver up to $t_{\rm final} = 25$ zs [10, 16]. The initial state is constructed as a Gaussian superposition of GCM states such the average energy is about 1 MeV above the saddle point.

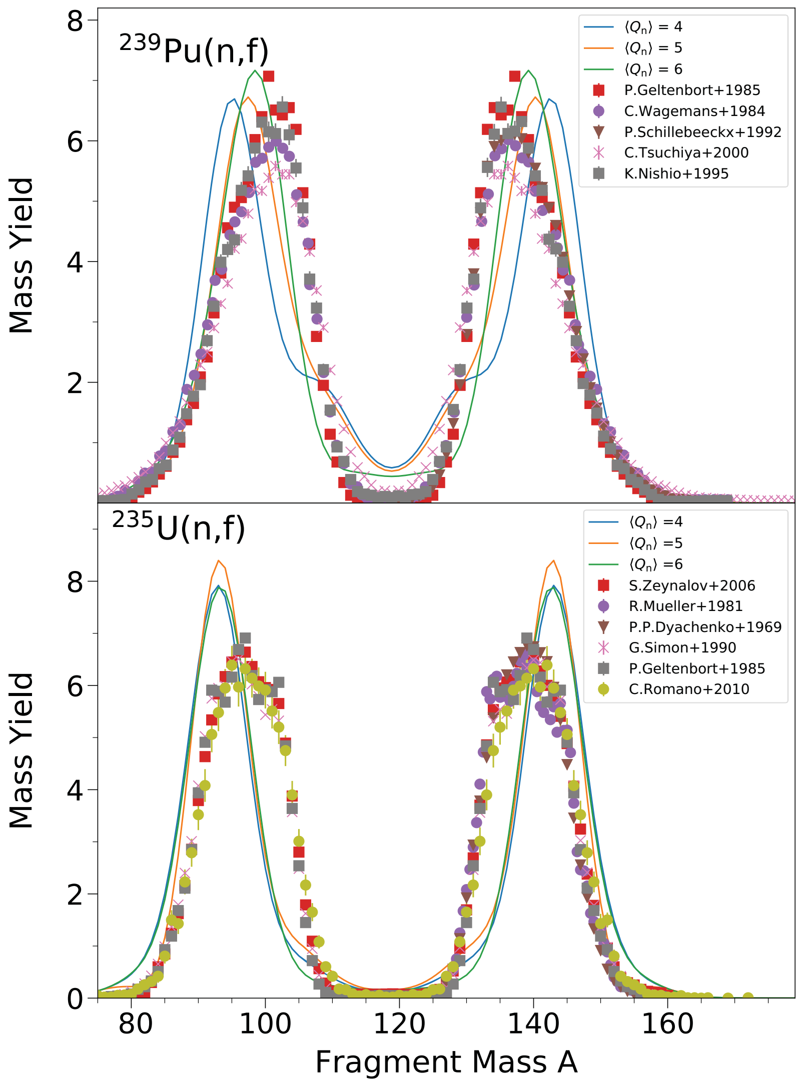

Figure 2. Initial fission fragment mass distributions for the ^{239}Pu(n,f) (top) and ^{235}U(n,f) (bottom) thermal fission. Calculations for three different different definitions of the scission line are compared with existing data from the EXFOR database.

Figure 2 shows the resulting mass distributions for both actinide nuclei. The results for ^{239}Pu are rather good and do not show too much variation with the definition of scission. The case of ^{235}U is not nearly as good as the yields are too narrow and too widely separated. This suggests that the collective space is too small: since mass yields are normalized, fragmentations missing from the scission line lead to artificially higher yields elsewhere. This problem was already identified in [17], where it was suggested that (q_{20}, q_{30}) should be replaced by collective variables more closely aligned with the number of particles in the fragments.

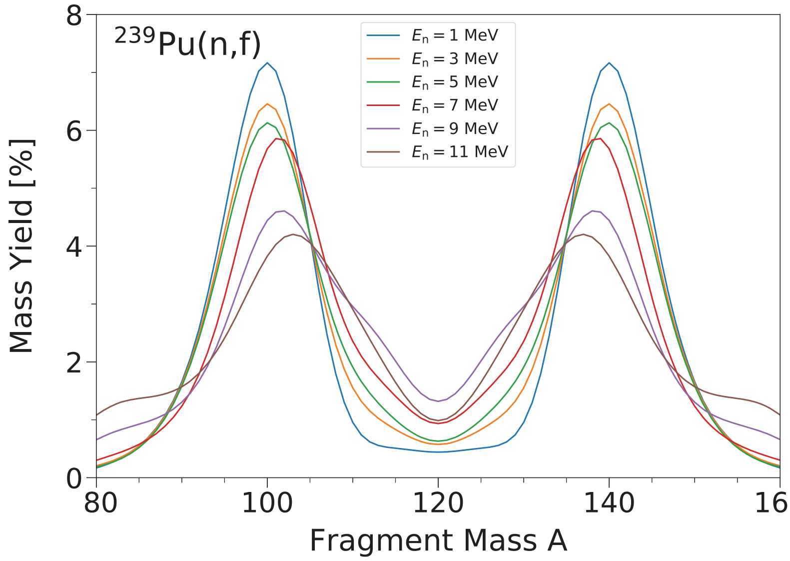

Figure 3. Initial fission fragment mass distributions for the ^{239}Pu(n,f) fission as a function of the incident neutron energy.

In the TDGCM+GOA, one can simulate increasing neutron energies E_n by simply increasing the collective energy, that is, the expectation value of the TDGCM+GOA collective Hamiltonian, $E_n \approx E_{\text{col}} - E_{\text{saddle}}$, with E_{saddle} the HFB energy of the saddle point. Figure 3 shows the evolution of the initial yields as a function of the neutron energy for ^{239}Pu(n,f). These results are qualitatively similar to earlier calculations by Younes and Gogny [17] and compatible with expectations: as the available excitation energy increases, the distribution becomes more symmetric. Although this result is encouraging, it is important to bear in mind that it contains a number of important approximations, which we discuss in more details in the next section.

4 Discussion

Because of the complexity of the fission process, calculations (whether microscopic or not) have a rather large uncertainty budget. In this section, we wish to discuss briefly some of the shortcomings of the particular calculations reported here, especially since there has been progress in addressing some of them.

There is a large consensus in the theory community that the PES is perhaps the most important ingredient in fission calculations [18]. Whether the initial yields are symmetric or asymmetric can be simply determined by whether the least-energy fission pathway goes through reflection-asymmetric shapes (in our calculations, characterized by $Q_{30} \neq 0$). However, these PES clearlt depend on the underlying energy functional. There has recently been much progress in rigorously quantifying the uncertainties associated with the functional [19–21]. Obviously, the PES also depends on the choice of the collective degrees of freedom. While the PES of Fig. 1 only involves collective coordinates, its physics content could be improved, e.g. by including pairing degrees of freedom [22–25]. Progress in computing facilities, combined with publicly available and carefully benchmakred DFT solvers [13, 26] provide more options to solve the HFB equations across an entire PES and handle the issue of its discontinuities [27].

Given the PES, the calculation of the initial yields within the TDGCM+GOA requires in addition full specification of (i) and collective inertia tensor, (ii) scission configurations and (iii) fission fragment properties.

- As discussed early on, scission is not a well-defined concept and there exist several possible definitions [14, 15, 28, 29]. Here we chose a simple criterion based on the size of the neck: as shown in Fig.2, it has a measurable impact on the yield, which could be quantified more rigorously.
- The theory of collective inertia has a long history; see, e.g. [30–34] for a selection of historical review papers on the subject. Recent benchmarks showed that fission observables such as spontaneous fission half-lives are highly sensitive to the approximation used to calculate the tensor B [35].
- Fission fragment properties are in principle determined at scission. In “adiabatic” theories such as the current implementation of the TDGCM+GOA, these properties are not always well predicted. Just before scission, the two prefragments are strongly entangled, leading to some arbitrariness in determining the excitation energy of the fragments [14, 15]; conversely, just after scission, the fragments are cold, contrary to experimental evidence. Going beyond these limitations requires explicit treatment of non-adiabatic effects, which have recently shown great potential [25, 36–40]. In the particular case of particle number, recent applications of projection techniques show great promise to improve the precision of charge and mass yields [41].

Extending the TDGCM+GOA at increasing excitation energy of the compound nucleus opens another Pandora’s box of interesting problems. First of all, it is not at all clear what is the best approach to describe the system at excitation energies of the order of 10-20 MeV, where the level density if extremely high: direct approaches where generator states include quasiparticle excitations are still in their infancy and would need to be severely truncated [42]; a finite-temperature formalism poses conceptual problems, both in terms of relating the temperature to the excitation energy [43], and for defining a collective wave function [44]. In the calculations shown in Fig.3, these effects were not taken into account: both the PES and the collective inertia were computed at zero-temperature.

5 Conclusion

In this paper, we report some benchmark calculations of the initial mass yields in the neutron-induced fission of the two major actinides ^{239}Pu and ^{235}U. We compare yields for thermal neutrons with experimental data and show the evolution of the yields as a function of neutron energy. Finally, we discuss some of the theoretical challenges in improving the fidelity of the models.

This work was performed under the auspices of the U.S. Department of Energy by Lawrence Livermore National Laboratory under Contract DE-AC52-07NA27344.

References

[1] N. Schunck, L.M. Robledo, Rep. Prog. Phys. **79**, 116301 (2016)
[2] N. Schunck, *Energy Density Functional Methods for Atomic Nuclei.*, IOP Expanding Physics (IOP Publishing, Bristol, UK, 2019), ISBN 978-0-7503-1423-7, oCLC: 1034572493
[3] J.F. Berger, in *Dynamics of Wave Packets in Molecular and Nuclear Physics*, edited by J. Broeckhove, L. Lathouwers, P. van Leuven (Springer Berlin Heidelberg, 1986), Number 256 in Lecture Notes in Physics, p. 21, ISBN 978-3-540-16772-3 978-3-540-39847-9
[4] J.F. Berger, M. Girod, D. Gogny, Comput. Phys. Commun. **63**, 365 (1991)
[5] H. Goutte, P. Casoli, J.F. Berger, Nucl. Phys. A **734**, 217 (2004)
[6] H. Goutte, J.F. Berger, P. Casoli, D. Gogny, Phys. Rev. C **71**, 024316 (2005)
[7] D. Regnier, M. Verrière, N. Dubray, N. Schunck, Comput. Phys. Commun. **200**, 350 (2016)
[8] D. Regnier, N. Dubray, N. Schunck, M. Verrière, Phys. Rev. C **93**, 054611 (2016)
[9] D. Regnier, N. Dubray, M. Verrière, N. Schunck, Comput. Phys. Commun. **225**, 180 (2018)
[10] D. Regnier, N. Dubray, N. Schunck, Phys. Rev. C **99**, 024611 (2019)
[11] J. Bartel, P. Quentin, M. Brack, C. Guet, H.B. H{\aa}kansson, Nucl. Phys. A **386**, 79 (1982)
[12] W. Satuła, J. Dobaczewski, W. Nazarewicz, Phys. Rev. Lett. **81**, 3599 (1998)
[13] N. Schunck, J. Dobaczewski, W. Satuła, P. Bączyk, J. Dudek, Y. Gao, M. Konieczka, K. Sato, Y. Shi, X.B. Wang et al., Comput. Phys. Commun. **216**, 145 (2017)
[14] N. Schunck, D. Duke, H. Carr, A. Knoll, Phys. Rev. C **90**, 054305 (2014)
[15] W. Younes, D. Gogny, Phys. Rev. Lett. **107**, 132501 (2011)
[16] D. Regnier, D. Lacroix, G. Scamps, Y. Hashimoto, Phys. Rev. C **97**, 034627 (2018)
[17] W. Younes, D. Gogny, Tech. Rep. LLNL-TR-586678, Lawrence Livermore National Laboratory (LLNL), Livermore, CA (2012)
[18] P. Möller, D. Madland, A.J. Sierk, A. Iwamoto, Nature **409**, 785 (2001)
[19] J. Dobaczewski, W. Nazarewicz, P.G. Reinhard, J. Phys. G: Nucl. Part. Phys. **41**, 074001 (2014)
[20] N. Schunck, J.D. McDonnell, J. Sarich, S.M. Wild, D. Higdon, J. Phys. G: Nucl. Part. Phys. **42**, 034024 (2015)
[21] N. Schunck, J.D. McDonnell, D. Higdon, J. Sarich, S.M. Wild, Eur. Phys. J. A **51**, 1 (2015)
[22] J. Sadhukhan, J. Dobaczewski, W. Nazarewicz, J.A. Sheikh, A. Baran, Phys. Rev. C **90**, 061304 (2014)
[23] J. Zhao, B.N. Lu, T. Nikšić, D. Vretenar, S.G. Zhou, Phys. Rev. C **93**, 044315 (2016)
[24] R. Bernard, S.A. Giuliani, L.M. Robledo, Phys. Rev. C **99**, 064301 (2019)
[25] A. Bulgac, S. Jin, K.J. Roche, N. Schunck, I. Stetcu, Phys. Rev. C **100**, 034615 (2019)
[26] R.N. Perez, N. Schunck, R.D. Lasseri, C. Zhang, J. Sarich, Comput. Phys. Commun. **220**, 363 (2017)
[27] N. Dubray, D. Regnier, Comput. Phys. Commun. **183**, 2035 (2012)
[28] K.T.R. Davies, R.A. Managan, J.R. Nix, A.J. Sierk, Phys. Rev. C **16**, 1890 (1977)
[29] N. Dubray, H. Goutte, J.P. Delaroche, Phys. Rev. C **77**, 014310 (2008)
[30] R.E. Peierls, J. Yoccoz, Proc. Phys. Soc. A **70**, 381 (1957)
[31] F. Villars, Nucl. Phys. A **285**, 269 (1977)

[32] M. Baranger, M. Veneroni, Ann. Phys. **114**, 123 (1978)
[33] P.G. Reinhard, K. Goeke, Rep. Prog. Phys. **50**, 1 (1987)
[34] M. Matsuo, T. Nakatsukasa, K. Matsuyanagi, Prog. Theor. Phys. **103**, 959 (2000)
[35] J. Sadhukhan, K. Mazurek, A. Baran, J. Dobaczewski, W. Nazarewicz, J. Sheikh, Phys. Rev. C **88**, 064314 (2013)
[36] C. Simenel, A.S. Umar, Phys. Rev. C **89**, 031601(R) (2014)
[37] G. Scamps, K. Hagino, Phys. Rev. C **91**, 044606 (2015)
[38] Y. Tanimura, D. Lacroix, G. Scamps, Phys. Rev. C **92**, 034601 (2015)
[39] A. Bulgac, P. Magierski, K.J. Roche, I. Stetcu, Phys. Rev. Lett. **116**, 122504 (2016)
[40] Y. Tanimura, D. Lacroix, S. Ayik, Phys. Rev. Lett. **118**, 152501 (2017)
[41] M. Verrière, N. Schunck, T. Kawano, Phys. Rev. C **100**, 024612 (2019)
[42] R. Bernard, H. Goutte, D. Gogny, W. Younes, Phys. Rev. C **84**, 044308 (2011)
[43] N. Schunck, J.D. McDonnell, D. Higdon, J. Sarich, S. Wild, Nucl. Data Sheets **123**, 115 (2015)
[44] K. Dietrich, J.J. Niez, J.F. Berger, Nucl. Phys. A **832**, 249 (2010)